Fabrication of an All-polysaccharide Composite Film from Hemicellulose and Methylcellulose

Gui-Chun Hu,[a,b,]* Shiyu Fu,[c] Fuqiang Chu,[a,b] and Guangyuan Wu [a,b]

There is significant interest in preparing packaging film from sustainable polysaccharides, especially hemicellulose (HC). Hemicellulose isolated from wheat straw tends to aggregate into dissolved particles in aqueous solutions and to form poor films. When methylcellulose (MC) was added into the HC solution, HC and MC formed a HC-MC complex. With increased MC content, the size of the HC-MC complex decreased, and its surface charge increased at the same time. When 35 wt% MC was added into the HC, a continuous HC-MC film formed in the layer structure. The HC-MC film with 75 wt% MC showed a more compact layer structure compared with other films. The tensile strengths of the HC-MC film increased with the MC addition. When MC was added to 75 wt%, the tensile strengths of the HC-MC film reached their maximum values, which were higher than that of MC film. This high film strength suggested these HC-MC composite films have potential applications in packaging material.

Keywords: Hemicellulose; Methylcellulose; Composite film; Interaction; Morphology; Tensile strength

Contact information: a: School of Light Industry and Engineering, Qilu University of Technology, Shandong Province, Jinan, 250353, P.R. China; b: Key Laboratory of Green Printing & Packaging Materials and Technology in Universities of Shandong, Qilu University of Technology, Shandong Province, Jinan, 250353, P.R. China; c: State Key Laboratory of Pulp and Paper Engineering, South China University of Technology, Guangzhou, 510640, P.R. China;
** Corresponding author: hu2004326431@163.com*

INTRODUCTION

Coupled with the increasing scarcity of natural fossil fuels, waste disposal of nonbiodegradable plastic-based packaging materials raises considerable environmental and supply concerns (Schnell *et al.* 2017). The use of lignocellulose resources, such as agricultural wastes, are becoming an attractive alternative due to their renewable origin, biodegradability, and non-human food application (Mikkonen *et al.* 2009; Alekhina *et al.* 2014; Gordobil *et al.* 2014). In addition, agricultural residues are produced in large quantities every year, and most are discarded and burned with no value (Gordobil *et al.* 2014). Hemicellulose (HC), the second most abundant polysaccharide in lignocellulose, has shown great potential in bio-based and biodegradable packaging materials because its film has good barrier properties against oxygen and oils at low or moderate relative humilities (Alekhina *et al.* 2014; Gordobil *et al.* 2014). However, pure HC always forms a brittle film because of its low molecular weight, high glass transition temperature, and low solubility in water (Schnell *et al.* 2017; Gordobil *et al.* 2014). To improve HC film formation, HC based composite materials with the external plasticizers (*e.g.*, sorbitol, xybitol) have been developed (Mikkonen *et al.* 2009; Gordobil *et al.* 2014). Even with the plasticizers, the mechanical properties of HC composite films are less than desirable (Mikkonen *et al.* 2012; Ayoub *et al.* 2013; Stepan *et al.* 2014).

Cellulose, the main polysaccharide component of lignocellulose, has been widely used as reinforcement for polymer composite films due to its high strength properties (Gordobil *et al.* 2014; Stevanic *et al.* 2014). It has been added in HC composite film to improve the film strength properties (Gordobil *et al.* 2014; Stevanic *et al.* 2014). However, high amounts of plasticizers, such as glycerol and sorbitol, should be added into the HC composite film to improve film formability (Hansen *et al.* 2012). Methylcellulose (MC), a cellulose ether, exhibits excellent film-forming properties and has been widely used as an additive to non-film-forming substance, such as silver, chitosan, and NaA zeolite membrane, to form continuous films (Peressini *et al.* 2003; Maity *et al.* 2012; Kanimozhi *et al.* 2016; Abdullah *et al.* 2017; Wei *et al.* 2017). In the plant cell wall, HC is tightly associated with cellulose fibrils, forming the unique natural composite structure (Stevanic *et al.* 2014). In addition, *in vitro* HC adsorbs irreversibly on the cellulose fiber surface (Ostlund and Brelid 2011). Based on the arrangement of HC and cellulose, coupled with the unique characteristics of MC, a novel strategy for forming HC composite film was prepared by combining HC and MC. The interactions between HC and MC, as well as the influences of MC on the properties of composite films, were investigated.

EXPERIMENTAL

Preparation of HC

The HC extraction method was previously described (Hu *et al.* 2015). The air-dried wheat straw was ground and screened. The fraction passing through a 40-mesh and retained on an 80-mesh screen was delignified with sodium chlorite in acidic conditions for 3 h. The residue was mixed with 5 g/L sodium hydroxide and stirred for 10 h at 30 °C. After the suspension was filtered, the filtrate was neutralized with hydrochloric acid and then mixed with triple-volume ethanol. After a centrifugation step, the precipitate was washed with 95% ethanol and dried under a vacuum to obtain the HC source. The yield of HC was roughly 14%.

Once extracted, the HC was dissolved in deionized water to obtain a 0.015 g/mL HC solution. The HC solution was mixed with 4.4 mL of deionized water and 0.3 mL of 72% H_2SO_4, then hydrolyzed for 1 h at 121°C. The hydrolysate was analyzed on a Dionex HPLC system (ICS-3000, *Dionex* Corp., Sunnyvale, CA, USA) equipped with an electrochemical detector and a PA20 column.

Interactions between HC and MC Analyzed by Dynamic Light Scattering

The MC (29.4% methoxyl content, average molecular mass 21000 Da) was purchased from AoChi Biotechnology Co. Ltd. (Hunan, China). It was dispersed in deionized water (pH=6.8) at 75 °C with continuous stirring until completely dissolved. Then the MC solution was cooled at room temperature (28 °C) to obtain a transparent 0.015 g/mL MC solution. The sizes and zeta potentials of HC and MC were measured by a Dynamic light scattering (DLS) analyzer equipped with a laser Doppler microelectrophoresis (Zetasizer Nano ZS90, Malvern Instruments, Malvern, UK). In addition, the MC and HC complex solution was prepared by varying the solid MC content to investigate the physical size and zeta potential, and thereafter to estimate the stability of the MC and HC interaction. The solid MC content was 6.5, 12.0, 22.0, 35.0, 45.0, 50.0, and 75.0 wt% of the total mixture of HC and MC. The total MC and HC complex solution volume is consistent.

Film Preparation

Composite films were prepared using the conventional solution casting technique. Solutions of HC and MC were mixed by weight percentage with continuous stirring for 10 min at room temperature. The complex solution was cast into polystyrene petri dishes (9.00 cm in radius) and placed in the controlled conditions (23 °C and 50% relative humidity (RH)) to facilitate solvent evaporation. The films were peeled and stored in sealing bags.

Film Characteristics

The thickness of the composite film was measured using a thickness tester (L&W Micrometer, Lorentzen Wettre, Sweden). The film density was calculated from the thickness and weight of the film samples. Scanning electron microscopy (SEM) images were collected on a Hitachi S-570 (Tokyo, Japan) microscope at an accelerating voltage of 20 kV.

The tensile strength, tensile strain at break, and Young's modulus of the films were determined using an Instron 4411 mechanical property tester with a 500-N load cell (Instron Ltd., Norwood, MA, USA). The initial grip distance was 25 mm, and the rate of grip separation was 5 mm min^{-1}. The specimens were 10 mm wide and approximately 70 mm long.

RESULTS AND DISCUSSION

The Size and Zeta Potential of HC and MC

The size distributions of HC and MC were analyzed with DLS as shown in Fig. 1. The size distribution of HC was unimodal, and the average peak size was 684 nm. Xylan was the predominant polysaccharide component, comprising 77% of the relative carbohydrate in HC (Table 1). There was also a considerable content of arabinose (17.4%), but only small amounts of glucose (3.2%) and galactose (2.1%). Therefore, HC has xylan backbones with different side chains such as arabinose, glucose, and galactose. The arabinose/xylose ratio was 0.22, which indicates that the side chain along the xylan main chain is low. Weakly substituted HC tends to aggregate (Chaa *et al*. 2008; Zhang *et al.* 2011). Kabel *et al.* (2007) studied the solubility behavior of xylan hemicelluloses with DLS and found that xylan hemicelluloses with minimal substituents tended to aggregate. Thus, it was deduced that virgin HCs interacted with each other through the xylan main chain and formed aggregations.

The size distribution of MC at 28 °C was also unimodal, and the average size was 128 nm. At high concentrations (above 0.0005 g/mL) and low temperatures, MC exists in the form of individual coils and clusters (Kobayashi *et al.* 1999; Lagaron and Fendler 2009). The size distribution of MC is also accordance with the research of Wei *et al.* (2017).

Table 1. Sugar Composition of HC

Sample	Total Sugars (% w/w)	Relative Carbohydrate Composition (% w/w)				
		Arabinose	Xylose	Galactose	Glucose	Arabinose/Xylose
HC	96%	17.4	77.0	2.1	3.2	0.22

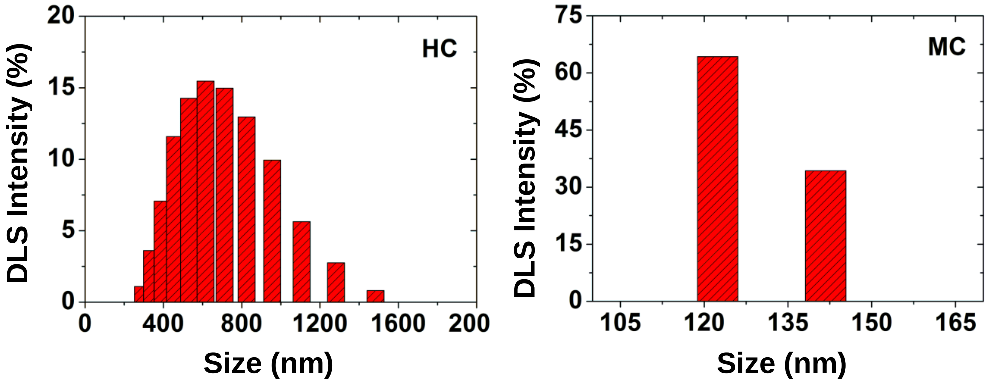

Fig. 1. The size distributions of HC and MC

The zeta potentials of HC and MC in deionized water at 28 °C were -20 and -70 mV, respectively (Table 2); the surface charge of MC was higher than that of HC. The conductivity of MC dissolved in deionized water (1.4 mS/cm) was also higher than that of HC (0.6 mS/cm). Hemicellulose contains hydroxyl group in the xylan backbone and side chains; however, methylcellulose contains methyl groups and hydroxyl groups, which increases the surface charge of MC.

Table 2. Zeta Potential and Conductivity for HC and MC

Sample	Zeta Potential (mV)	Conductivity (mS/cm)
HC	-20	0.6
MC	-70	1.4

The Interactions between HC and MC

To verify the interactions between HC and MC, the size distribution and surface charge of the MC and HC complex solutions with different mass fraction were investigated using DLS at 28 °C, as shown in Fig. 2. When the MC content increased to 12 wt%, the average peak size reached the maximum value at 1576 nm, which was much larger than the sizes of HC and MC. In the plant cell wall or *in vitro*, HC adsorb onto cellulose through hydrogen bonding and/or chain arrangement (Eronen *et al.* 2011; Kohnke *et al.* 2011). Therefore, it was deduced that individual MC is completely covered by HC aggregates to form the HC-MC complex. By continually increasing the MC content, the HC-MC complex sizes decreased, as in the case of MC content at 35 wt%, where the average peak size decreased to 289 nm. This value is much smaller than that of pure HC aggregation but larger than that of MC. When the MC content in the complex reached 75 wt%, the average peak size decreased to 179 nm and is close to the size of MC. This phenomenon indicates that HC is separated from the aggregation formation and redistributed on the MC surface.

The zeta potential of the HC-MC complex in an aqueous solution initially became more negative with an increase in the MC content (Fig. 2). At 75 wt% MC content, the zeta potential reached its most negative value at -95 mV. Continuing to increase the MC content allowed the zeta potential of complex to recover, nearly reaching the zeta potential of MC. The conductivity of the HC-MC complex increased with the addition of MC to a maximum value (2.7 mS/cm) at 75 wt% MC content. This might be caused by the HC separation from the aggregates, which leads to an increase in the proportion of hydrogen and carboxyl groups.

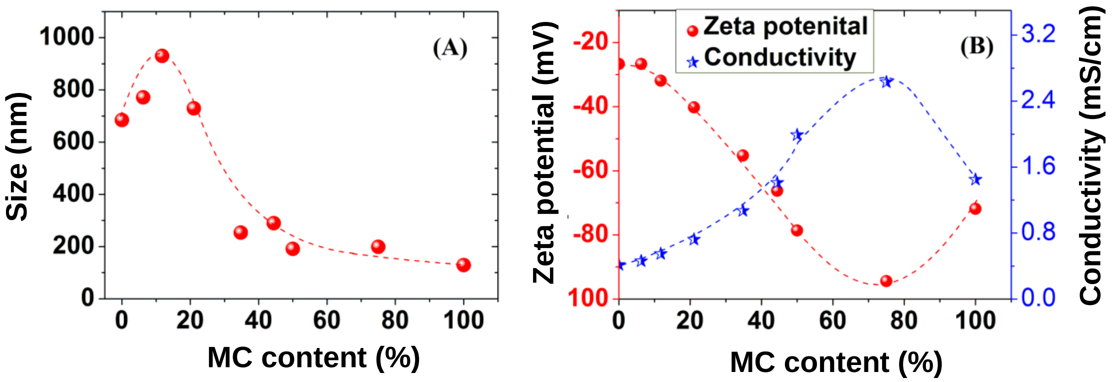

Fig. 2. The size distributions and zeta potential of the HC-MC complex with different MC contents. Different volume MC solution (concentration 0.015 g/ml) was added into HC solution (concentration 0.015 g/ml). The total MC and HC complex solution volume is consistent.

The interaction mechanism between HC and MC was deduced, as shown in Fig. 3. Hemicellulose shows as an aggregation formation tendency with a hydrophobic core consisting of a cross-linked xylan main chain with all side chains relocated to or near the core surface to facilitate interaction with the aqueous surroundings. Methylcellulose is a structure of individual fiber. At low MC content, such as 6.5 wt% and 12 wt%, the MC surface is totally covered by HC in aggregation formation to form the HC-MC complex (as shown in Fig. 3a), which leads to an increase in the average size. With the increase of MC content in the complex solution, such as at 22 wt%, 35 wt%, and 50 wt%, HC aggregations starts to disaggregate and redistribute on the MC surface as shown in Fig. 3b, resulting in the decrease of HC-MC complex size and an increase in surface charge. When enough MC is present, such as at 75 wt% MC content, HC separates from the aggregation into monomers and adsorbs on the celluloses' surface in the formation of loops and tails (shown in Fig. 3c), which leads to an increase in surface charge. This phenomenon is consistent with studies by Kabel *et al.* (2007) and Gu and Catchmark (2013). With excess MC in the complex, above 75 wt% MC content, the HC monomer interacts several times with the MC surface, resulting in an almost linearly adsorbed polymer train as shown in Fig. 3d.

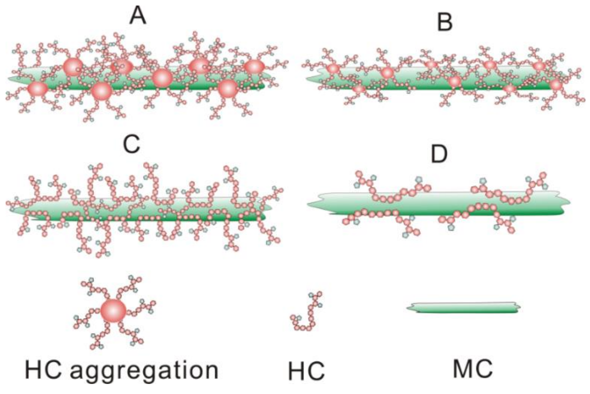

Fig. 3. The interaction mechanism between HC and MC. a) Original HC aggregations adsorbed on the MC surface; b) Disaggregated HC aggregations adsorbed on the MC surface; c) HC monomers adsorbed on the MC surface in the formation of loops and tails; and d) HC monomers linearly adsorbed on the MC surface

The Formation of HC - MC Composite Film

The composite films from HC and MC are shown in Table 3. As expected, the pure MC shows good film-forming properties and forms a continuous and transparency film. The pure HC could not produce continuous film, which is in agreement with previous studies (Kayserilioglu *et al.* 2003; Goksu *et al.* 2007). The addition of MC could improve the HC film formation and it is necessary to use of 35 wt% MC to form a film without cracks.

One of the possible explanations for poor HC film forming ability is that HC forms in aggregate in deionized water. In addition, HC properties, such as insufficient chain length and high glass transition temperature, contribute to this phenomenon (Gröndahl *et al.* 2004). The addition of MC could separate HC from the aggregate formation and then adsorb HC, which would improve the HC film formation.

Table 3. Optical Images of HC-MC Composite Films

HC film	MC film	HC-35%MC [a] composite film
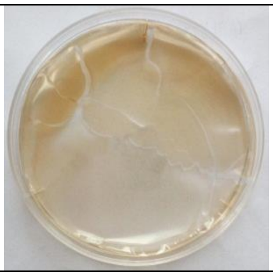	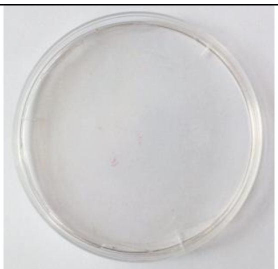	

[a] HC-35%MC composite film represents the HC-MC composite film with 35 wt% content.

Morphology of the HC-MC Composite Films

SEM cross-section micrographs of the HC-MC composite films with different MC content are shown in Fig. 4, where the microstructure can be observed from the surface through the interior of the films.

The cross-section of pure HC film is continuous with some particles, whereas the cross-section of pure MC film exhibits a clear layered structure. The addition of MC introduces the lamellar structure into the HC-MC composite films, as demonstrated in the HC-35% MC composite film. For the HC-75% MC composite film, the layers are closely connected to each other (Fig. 4).

The density study of the HC-MC composite film showed that with the introduction of additional MC, the density of the HC-MC composite film increased obviously (as shown in Fig. 5). When the MC content reached 75%, the density of the HC-MC composite film reached its maximum value (Fig. 5).

As mentioned in the previous section, MC adsorbs on the HC at high MC content, and HC contains more side chains and less crystallinity compared to cellulose (Hu *et al.* 2015). Methylcellulose adsorbed hemicellulose increases the hydrogen bonds in the HC-MC composite film and could increase the rate of connection among layers in the composite film.

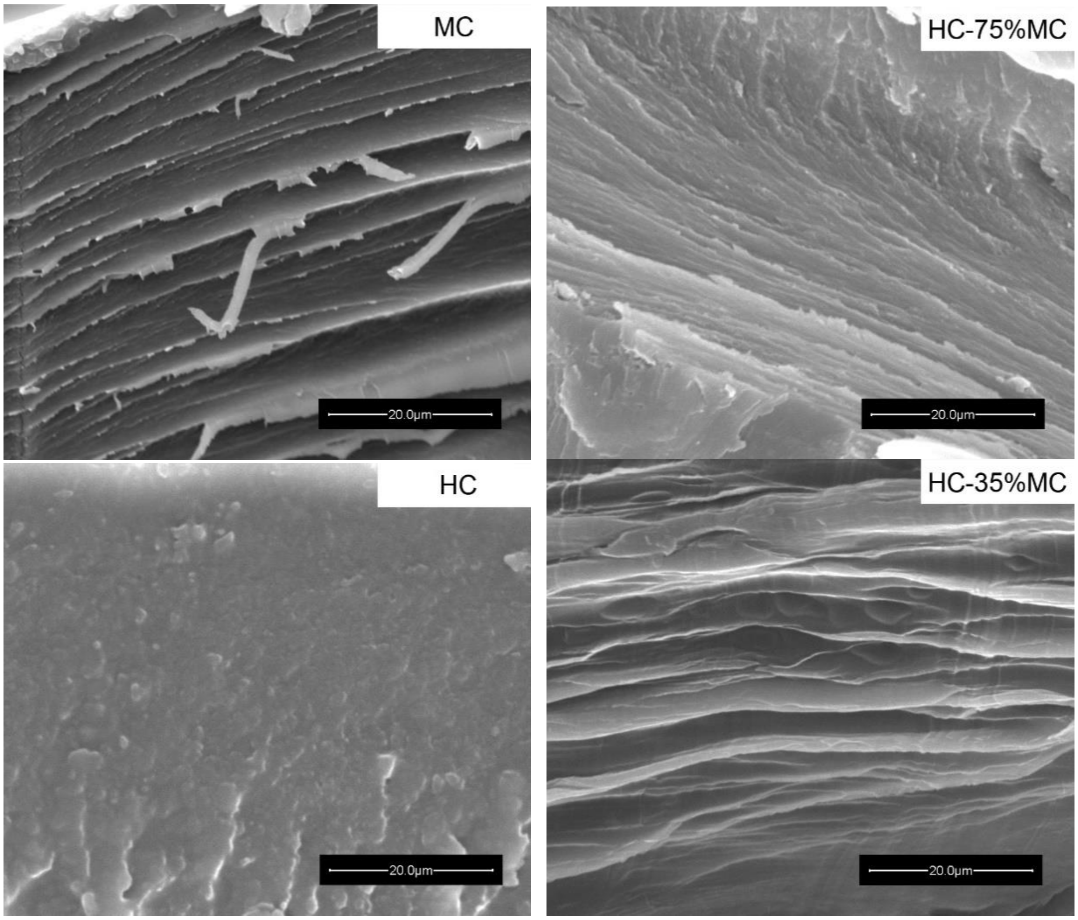

Fig. 4. The SEM cross-section micrographs of HC-MC composite films with different MC content. HC represents the pure HC film; MC represents the pure MC film; HC-35% MC and HC-75% MC represent the HC-MC composite films with 35 wt% MC and 75 wt% MC, respectively.

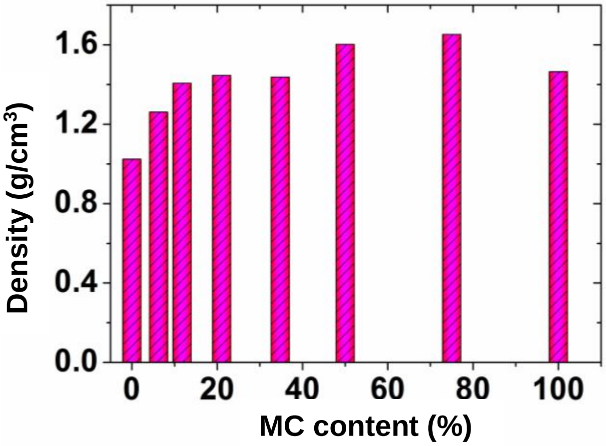

Fig. 5. The density of HC-MC composite films with different MC contents

Mechanical Properties

The mechanical properties, such as tensile strain, tensile strength, and Young's modulus of the HC-MC composite films and the virgin MC film were measured at conditions of 50% RH and 25 °C. Figure 6 shows the appearance and representative stress-strain curves of both the HC-MC composite films and the virgin MC film. The

Young's modulus, tensile strain, and tensile strength are summarized in Table 4. Adding more MC improved the mechanical properties of the HC-MC composite film. For example, increasing the amount of MC in HC-MC composite films from 35% to 50% resulted in an increase in the stress response (from 39.0 to 39.9 MPa), accompanied by increases in the tensile strain at break (from 3.25 to 3.5%), and Young's modulus (from 1472 to 1891 MPa). However, the tensile strengths of the HC-MC composite films at MC contents from 35% to 50% were lower than the virgin MC film. It was hypothesized that at low MC contents, HC in aggregate formation fully covered the surface of MC and interrupted the strong cellulose interactions. With an increase in MC, HCs were gradually and completely dispersed from the aggregation and adsorbed on the surface of MC with loops and tails. At 75 wt% MC content, the HC-MC composite film showed the best mechanical properties; the tensile strain, tensile strength, and Young's modulus increased to 15.6%, 87.2 MPa, and 2005 MPa, respectively. The hydrogen bonds in both inter-MC and HCs become the main bonding for the HC-MC composite film.

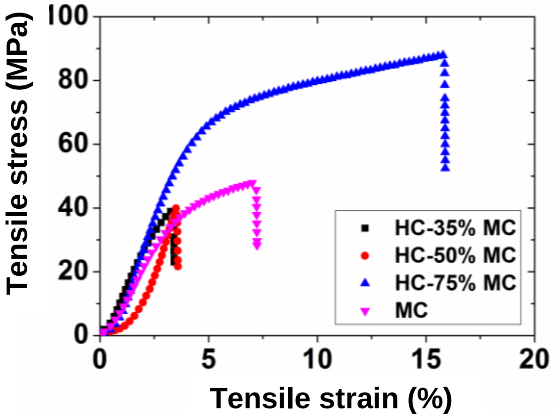

Fig. 6. Tensile stress-tensile strain curves of HC-MC composite films. HC-35% MC, HC-50% MC, and HC-75% MC represent the HC-MC composite films with 35 wt% MC, 50 wt% MC, and 75 wt% MC, respectively

Table 4. The Average Values of Tensile Stress, Tensile Strain, and Young's Modulus of Composite Film

Samples	HC-35%Mc	HC-50%Mc	HC-75%Mc	Mc
Tensile strength (MPa)	38.95	39.88	87.22	47.88
Tensile strain (%)	3.25	3.5	15.56	7.00
Young's modulus (MPa)	1472.2	1890.9	2005.5	1335.9

CONCLUSIONS

1. Pure hemicellulose (HC) isolated from wheat straw developed an aggregated form in aqueous solution and could not form continuous a film. Methylcellulose (MC) was added into the HC solution and adsorbed on HC to form a HC-MC complex.
2. With an increase in MC content, the size of the HC-MC complex decreased, and its surface charge increased. It is necessary to use 35 wt% of MC to form an HC-MC composite film without cracks.

3. The HC-MC composite films showed layer structures, and the layers of the HC-MC composite film with 75 wt% MC were more closely connected to each other compared to other HC-MC composite and virgin films. With the increase in MC content, the densities of HC-MC composite films increased, and at 75 wt% MC content, the density of the composite film reaches its maximum.
4. The tensile strengths of the HC film were all improved with the MC addition. The tensile strain, tensile strength, and Young's modulus of the HC-MC composite film with 75 wt% MC reached their maximum values. The prepared HC-MC composite films combined to have good film-forming and good mechanical properties, which could be potentially applied in food packaging areas.

ACKNOWLEDGEMENTS

The financial support of the Natural Science Foundation of Shandong Province (No. ZR2017PC020 and No.ZR2017LF027) is cheerfully acknowledged. The authors would like to thank the support of Key Research and Development Program of Shandong Province (No. 2018GGX106009) and Shandong Province Higher Educational Science and Technology Program (No.J17KA178) for their partial funding of this research.

REFERENCES CITED

Abdullah, O. G., Hanna, R. R., and Salman, Y. A. K. (2017). "Structural, optical, and electrical characterization of chitosan: methylcellulose polymer blends based film," *Journal of Materials Science: Materials in Electronics* 28(14), 10283-10294. DOI: 10.1007/s10854-017-6796-7

Alekhina, M., Mikkonen, K. S., Alen, R., Tenkanen, M., and Sixta, H. (2014). "Carboxymethylation of alkali extracted xylan for preparation of bio-based packaging films," *Carbohydrate Polymers* 100, 89-96. DOI: 10.1016/j.carbpol.2013.03.048

Ayoub, A., Richard, A. V., Pawlak, J. J., Sadeghifar, H., and Salam, A. (2013). "Development of an acetylation reaction of switchgrass hemicellulose in ionic liquid without catalyst," *Industrial Crops and Products* 44, 306-314. DOI: 10.1016/j.indcrop.2012.10.036

Chaa, L., Joly, N., Lequart, V., Faugeron, C., Mollet, J. C., Martin, P., and Morvan, H. (2008). "Isolation, characterization and valorization of hemicelluloses from aristida pungens leaves as biomaterial," *Carbohydrate Polymers* 74(3), 597-602. DOI: 10.1016/j.carbpol.2008.04.017

Eronen, P., Osterberg, M., Heikkinen, S., Tenkanen, M., and Laine, J. (2011). "Interactions of structurally different hemicelluloses," *Carbohydrate Polymers* 86(3), 1281-1290. DOI: 10.1016/j.carbpol.2011.06.031

Goksu, E. I., Karamanlioglu, M., Bakir, U., Yilmaz, L., and Yilmazer, U. (2007). "Production and characterization of films from cotton stalk xylan," *Journal of Agricultural and Food Chemistry* 55(26), 10685-10691. DOI: 10.1021/jf071893i

Gordobil, O., Egues, I., Urruzola, I., and Labidi, J. (2014). "Xylan-cellulose films: Improvement of hydrophobicity, thermal and mechanical properties," *Carbohydrate Polymers* 112, 56-62. DOI: 10.1016/j.carbpol.2014.05.060

Gröndahl, M., Eriksson, L., and Gatenholm, P. (2004). “Material properties of plasticized hardwood xylans for potential application as oxygen barrier films,” *Biomacromolecules* 5(4), 1528-1535. DOI: 10.1021/bm049925n

Gu, J., and Catchmark, J. M. (2013). “The impact of cellulose structure on binding interactions with hemicellulose and pectin,” *Cellulose* 20(4), 1613-1627. DOI: 10.1007/s10570-013-9965-8

Hansen, N. M. L., Blomfeldt, T. O. J., Hedenqvist, M. S., and Plackett, D. V. (2012). “Properties of plasticized composite films prepared from nanofibrillated cellulose and birch wood xylan,” *Celllulose* 19(6), 2015-2031. DOI: 10.1007/s10570-012-9764-7

Hu, G., Fu, S., Liu, H., and Lucia, L. A. (2015). “Adsorption of cationized eucalyptus heteropolysaccharides onto chemical and mechanical pulp fibers,” *Carbohydrate Polymers* 123, 324-330. DOI: 10.1016/j.carbpol.2015.01.057

Kabel, M. A., Borne, H., Vincken, J. P., Voragen, A. G. J., and Schols, H. A. (2007). “Structural differences of xylans affect their interaction with cellulose,” *Carbohydrate Polymers* 69(1), 94-105. DOI: 10.1016/j.carbpol.2006.09.006

Kanimozhi, K., Basha, S. K., and Kumari, V. S. (2016). “Processing and characterization of chitosan/PVA and methylcellulose porous scaffolds for tissue engineering,” *Materials Science and Engineering: C* 61, 484-491. DOI: 10.1016/j.msec.2015.12.084

Kayserilioglu, B. S., Bakir, U., Yilmaz, L., and Akkas, N. (2003). “Use of xylan, an agricultural by-product, in wheat gluten based biodegradable films: Mechanical, solubility and water vapor transfer rate properties,” *Bioresource Technology* 87(3), 239-246. DOI: 10.1016/S0960-8524(02)00258-4

Kobayashi, K., Huang, C., and Lodge, T. P. (1999). “Thermoreversible gelation of aqueous methylcellulose solutions,” *Macromolecules* 32(21), 7070-7077. DOI: 10.1021/ma990242n

Kohnke, T., Ostlund, A., and Brelid, H. (2011). “Adsorption of arabinoxylan on cellulosic surfaces influence of degree of substitution and substitution pattern on adsorption characteristics,” *Biomacromolecules* 12(7), 2633-2641. DOI: 10.1021/bm200437m

Lagaron, J. M. and Fendler, A. (2009). “High water barrier nanobiocomposites of methyl cellulose and chitosan,” *Journal of Plastic Film and Sheeting* 25(1), 47. DOI: doi.org/10.1177/8756087909335712

Maity, D., Mollick, M. M. R., Mondal, D., Bhowmick, B., Bain, M. K., Bankura, K., Sarkar, J., Acharya, K., and Chattopadhyay, D. (2012). “Synthesis of methylcellulose–silver nanocomposite and investigation of mechanical and antimicrobial properties,” *Carbohydrate Polymers* 90(4), 1818-1825. DOI: 10.1016/j.carbpol.2012.07.082

Mikkonen, K. S., Heikkinen, S., Soovre, A., Peura, M., Serimaa, R., Talja, R. A., Helen, H., Hyvonen, L., and Tenkanen, M. (2009). “Films from oat spelt arabinoxylan plasticized with glycerol and sorbitol,” *Journal of Applied Polymer Science* 114(1), 457-466. DOI: 10.1002/app.30513

Mikkonen, K. S., Pitkanen, L., Liljestrom, V., Bergstrom, E. M., Serimaa, R., Salmen, L., and Tenkanen, M. (2012). “Arabinoxylan structure affects the reinforcement of films by microfibrillated cellulose,” *Cellulose* 19(2), 467-480. DOI: 10.1007/s10570-012-9655-y

Schnell, C.N., Galván, M.V., Peresin, M.S., Inalbon, M.C., Vartiainen, J., Zanuttini, M.A., and Mocchiutti, P. (2017). “Films from xylan/chitosan complexes: Preparation and characterization," *Cellulose* 24(10), 4393-4403. DOI:10.1007/s10570-017-1411-x

Stepan, A. M., Ansari, F., Berglund, L., and Gatenholm, P. (2014). "Nanofibrillated cellulose reinforced acetylated arabinoxylan films," *Composites Science and Technology* 98, 72-78. DOI: 10.1016/j.compscitech.2014.04.010

Stevanic, J. S., Mikkonen, K. S., Xu, C., Tenkanen, M., Berglund, L., and Salmen, L. (2014). "Wood cell wall mimicking for composite films of spruce nanofibrillated cellulose with spruce galactoglucomannan and arabinoglucuronoxylan," *Journal of Materials Science* 49(14), 5043-5055. DOI: 10.1007/s10853-014-8210-7

Peressini, D., Bravin, B., Lapasin, R., Rizzotti, C., and Sensidoni, A. (2003). "Starch-methylcellulose based edible films: Rheological properties of film-forming dispersions," *Journal of Food Engineering* 59(1), 25-32. DOI: 10.1016/S0260-8774(02)00426-0

Wei, X. L., Liang, S., Xu, Y. Y., Sun, Y. L., An, J. F., and Chao, Z. S. (2017). "Patching NaA zeolite membrane by adding methylcellulose into the synthesis gel," *Journal of Membrane Science* 530, 240-249. DOI: 10.1016/j.memsci.2016.12.015

Zhang, Y., Pitkanen, L., Douglade, J., Tenkanen, M., and Remond, C. (2011). "Wheat bran arabinoxylans: Chemical structure and film properties of three isolated fractions," *Carbohydrate Polymers* 86(2), 852-859. DOI: 10.1016/j.carbpol.2011.05.036

Article submitted: March 18, 2019; Peer review completed: May 26, 2019; Revised version received: June 23, 2019; Accepted: June 24, 2019; Published: July 3, 2019.
DOI: 10.15376/biores.14.3.6716-6726